Smart Structures and Systems, Vol. 4, No. 2 (2008) 261-278
DOI: http://dx.doi.org/10.12989/sss.2008.4.2.261

Application of shape memory alloy prestressing devices on an ancient aqueduct

Christis Z. Chrysostomou*

Cyprus University of Technology, POBox 50329, 3603 Limassol, Cyprus

Andreas Stassis‡

Higher Technical Institute, POBox 20423, 2152 Nicosia, Cyprus

Themos Demetriou‡†

Heras 13, Nicosia, Cyprus

Karim Hamdaoui‡‡

University of Pavia, Via Ferrata, No. 1, 27100 Pavia, Italy

(Received June 16, 2007, Accepted October 4, 2007)

Abstract. The results of the application of shape memory alloy (SMA) prestressing devices on an aqueduct are presented in this paper. The aqueduct was built in 1747 to provide water to the city of Larnaca and to its port. Because of its importance to the cultural heritage of Cyprus, the aqueduct has been selected as one of the case-study monuments in the project Wide-Range Non-Intrusive devices toward Conservation of Historical Monuments in the Mediterranean Area (WIND-CHIME). The Department of Antiquities of Cyprus, acting in a pioneering way, have given their permission to apply the devices in order to investigate their effectiveness in providing protection to the monument against probable catastrophic effects of earthquake excitation. The dynamic characteristics of the structure were determined in two separate occasions and computational models were developed that matched very closely the dynamic characteristics of the structure. In this paper the experimental setup and the measured changes in the dynamic characteristics of the monument after the application of the SMA devices are described.

Keywords: health monitoring; shape-memory-alloy; monuments; masonry structure; seismic-protection; system-identification; model updating.

*Assistant Professor, Corresponding author, E-mail: christis@spidernet.com.cy
‡Lecturer, E-mail: astassis@hti.ac.cy
‡†Structural Engineer, E-mail: t.demetriou@cytanet.com.cy
‡‡Ph.D Student, E-mail: karim@unipv.it

1. Introduction

Any intervention in the structural system of ancient monuments should be such that it neither violates their form nor changes drastically their structural behavior and most importantly should be reversible. In addition, the materials to be used must be compatible with the ones the monument is constructed. Traditional seismic retrofitting techniques have the disadvantage that most of them violate the above conditions. An alternative to the above is the use of innovative seismic-protection techniques, such as shape memory alloy (SMA) based devices. Such devices can be made very inconspicuous and therefore not violating the form of the monuments and at the same time can be very effective in dissipating the energy generated by earthquakes and hence protect the monuments. Such techniques have been evaluated within the INCO-MED project, "Wide-Range Non-Intrusive devices toward Conservation of Historical Monuments in the Mediterranean Area," WIND-CHIME. The application of SMA and other innovative devices in protecting monuments are reported by Biritognolo, *et al*. (2000), Croci (2000), and Chrysostomou, *et al*. (2003, 2004 and 2005).

In this paper a literature review on shape memory alloys is briefly presented along with the characteristics of the SMA supplied by the last author team. In addition, the results of the system identification study, which includes measurements and computational models and is described by Chrysostomou, *et al*. (2004 and 2008), are presented briefly. Finally, the experimental results of the application of SMA prestressing devices on the monument are presented and discussed.

2. Shape memory alloys

The series of Nickel/Titanium alloys developed by Buehler and Wiley (1965) in the 60's, exhibited a special property allowing them to regain and remember their original shape, although being severely deformed, upon a thermal cycle. This remarkable characteristic became known as the shape memory effect, and the alloys that exhibit it were named shape memory alloys. Later, it was found that at sufficiently high temperatures, such materials also have the super-elasticity property: the recovery of large deformations during mechanical loading-unloading cycles performed at constant temperature

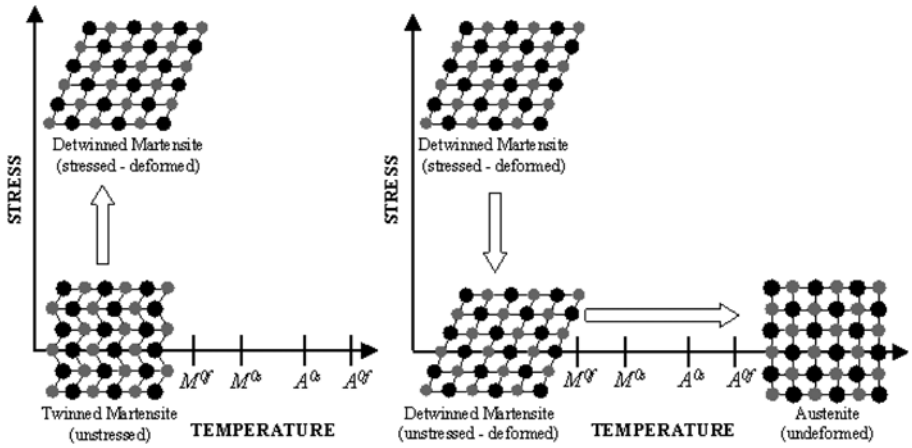

Fig. 1 Temperature-induced phase transformation and shape memory effect of SMA (Smartlab 2007)

(Auricchio 1995). Subsequently, SMAs lend themselves to innovative applications.

The SMAs have two stable phases: austenite at high temperature and, martensite at low temperature. In addition, the latter one (martensite) can be in one of two forms: twinned or de-twinned. If cooled, and in the absence of any applied load, the material transforms from austenite into twinned martensite phase. Here, no observable macroscopic shape change is seen. When the material in its martensitic phase is heated, a reverse phase transformation occurs and the material is transformed to the austenite phase. In Fig. 1, this process is illustrated and four characteristic temperatures are defined: i) M^{0s}, the martensitic start temperature (transformation from austenite to martensite); ii) M^{0f}, martensitic finish temperature (the material is fully in the martensitic phase); iii) A^{0s}, austenite start temperature (beginning of the reverse transformation, austenite to martensite); and iv) A^{0f}, austenite finish temperature (the material is in the austenitic phase).

A detailed references list on the use of SMA metals in different engineering applications is provided in the book Auricchio *et al*. 2001. The same book illustrates their use in vibration control in the form of austenitic wires. More recently, investigations are focused on the possibility of using the pre-stressed SMA wires to sew ancient buildings made by blocks (Casciati and Faravelli, 2004b and Casciati *et al*., 2005).

The mechanical characteristics of the Nickel/Titanium (abbreviated Nitinol or NiTi) alloys have already been widely investigated (Auricchio 2001, Saadat, *et al*. 2002 and Casciati 2003). Commercial products of Nitinol were already adopted in the retrofitting of a famous church (Auricchio, *et al*. 2001 and Saadat *et al*. 2002), and a numerical simulation when implementing the constitutive law of a commercial Ni-Ti alloy as a subroutine in the retrofitting of a large Egyptian monolithic statue, called the Memnon Colossus, were presented in Casciati and Osman (2005).

Because of their high cost and their limited range of potential transformation temperatures, the application of the NiTi alloy might not be the best candidate for the seismic retrofit of cultural heritage structures. Therefore, Casciati and Faravelli (2004a) checked the suitability of an alloy different from NiTi for the application in monumental retrofitting. The interest was focused on Copper-based SMA that consists of Cu, Al and Be chemical composites.

Several mechanical tests were also performed on this kind of alloy (Isalgue, *et al*. 2002, Faravelli and Casciati 2003, Casciati and Faravelli 2003 and Casciati and Faravelli 2004a), that was used, in the form of 2.85 mm wires, to reinforce a prototype of masonry wall to be tested in the laboratory (Delmonte 2007).

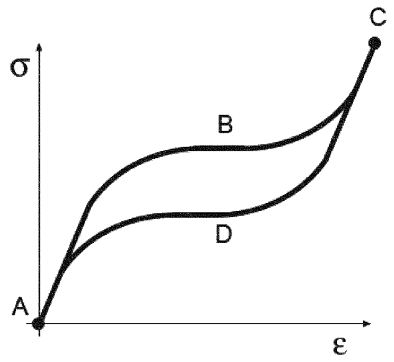

Fig. 2 Typical super-elasticity behaviour of SMA

In the loading-unloading stress strain curve shown in Fig. 2, the SMA material is first loaded (ABC), showing a nonlinear behaviour. Then, when unloaded (CDA), the reverse transformation occurs. This behaviour is hysteretic with no permanent strain (Auricchio *et al*. 1997). The pre-tensioned wires used in this study (3.5 mm diameter) are labeled AH140 and have the following values as chemical composition by weight:

$$\text{Al} = 11.8\%; \qquad \text{Be} = 0.5\%; \qquad \text{Cu} = 87.7\%$$

The producer provides the following transformation temperature:

$$M^{0s} = -18\ ^{o}\text{C};\ M^{0f} = -47\ ^{o}\text{C};\quad A^{0s} = -20\ ^{o}\text{C};\ A^{0f} = 2\ ^{o}\text{C}$$

The "M" and "A" mean here the martensite and austenite temperatures respectively, where the indices "s" and "f" denote respectively "start" and "finish".

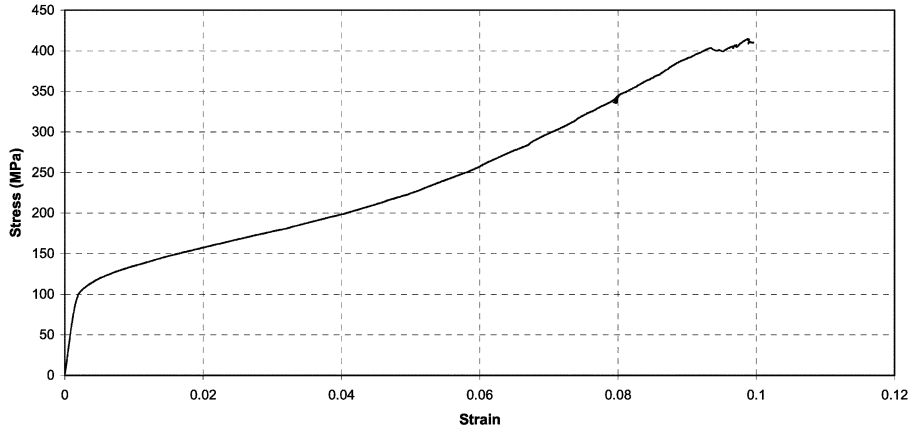

Fig. 3 Rupture test of a treated SMA at 50 ºC

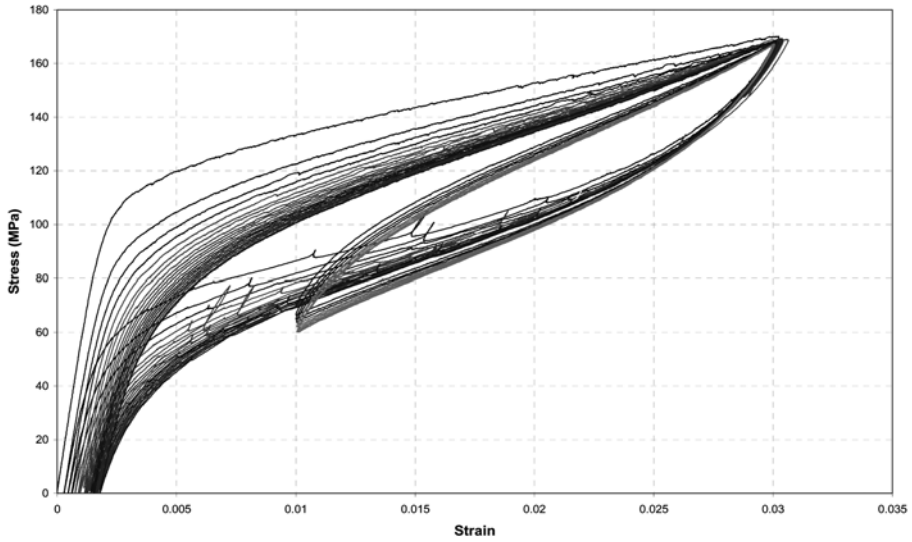

Fig. 4 Cycling of the 3.5 mm SMA wire: 20 cycles between 0 and 3% strain and 10 cycles between 1% and 3% strain

3. Characteristics of the SMA devices used in this research

The thermo-mechanical characteristics of the 3.5 mm diameter AH140 SMA wires used in this research are described by Casciati and Faravelli (2004). This type of alloy is selected on the basis of its typical temperature window, in which it maintains its super-elastic properties.

A basic aspect in managing the Cu Al Be alloy is the thermal treatment. Each SMA wire needs to be heated in an oven at 850 ºC for a time period that ranges between 1 and 5 minutes and depends on the specimen's cross section. The cooling to ambient temperature follows this process by direct immersion in water. To complete the process, the wires are treated for 120 minutes in an oven at 100 ºC, and then cooled again to ambient temperature. It is interesting to note that the thermal treatment has as an effect the reduction of the stress of the material from 500 MPa to about 250 MPa for the same strain of 6%.

Figure 3 gives the results of a rupture test of a 3.5mm diameter SMA wire at 50 ºC, while Fig. 4 a cyclic test of 20 cycles between 0 and 3% strain and 10 cycles between 1% and 3% strain. From the second graph it is clear that cycling between 1% and 3% results in a plateau with a centre at a strain of 2%.

Fig. 5 Rigid base to support the upper end of the SMA prestressing assembly

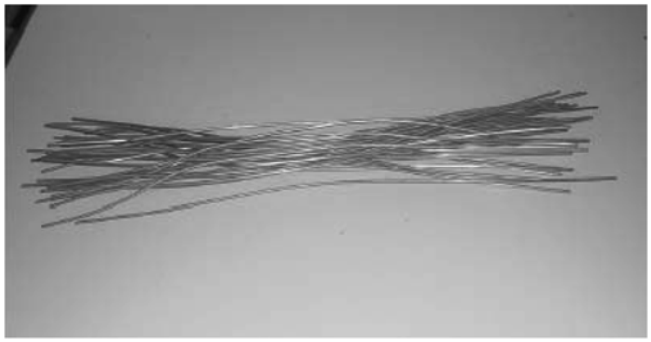

Fig. 6 Sixty centimeters long SMA wires of diameter 3.5 mm

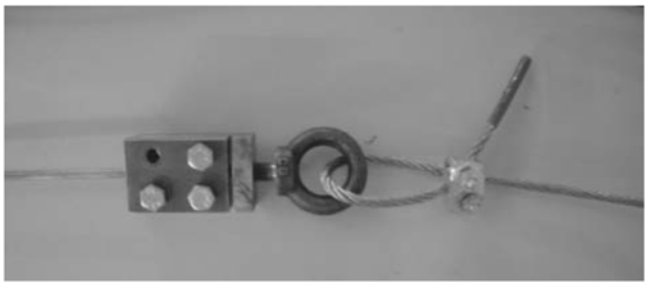

Fig. 7 Connection of the steel cable to the SMA wire

Fig. 8 Prestressing device

4. Experimental setup

After obtaining permission from the Antiquities Department of Cyprus for applying the SMA prestressing devices on the aqueduct, an effort was made to design the experiment in such a way so as to minimize any damage that the experiment would cause on the monument. For this reason it was decided to fix the wires at the base of one of the piers using bolts and at the top to support the wires on a rigid base (Fig. 5) that would transfer the force onto the aqueduct. This of course resulted in a setup that is not inconspicuous, but since this experiment was performed to test a hypothesis it is considered acceptable. In the event that such devices will be applied on the monument, then a discussion should be made with the Department of Antiquities to find the most inconspicuous way of applying the devices that would also serve the purpose of their application.

Fig. 9 SMA wires supported at the rigid base at the top of the pier of the aqueduct

Fig. 10 Prestressing devices used to apply tension in the assembly

Fig. 11 Bolts used to fix the assembly at the bottom of the pier

Twenty 60 cm long SMAs, as the ones shown in Fig. 6, were prepared by adding fixing devices at each of their ends. These devices were then connected to steel strands (Fig. 7) that extended from the top to the bottom of the pier of the aqueduct.

In order to be able to apply a prestressing force, the prestressing devices shown in Fig. 8 were used by placing them along the length of the steel strand. Two such devices were used for each strand, in order to be able to provide the required strain, taking into account the elongation of the SMA wire and that of the steel strand.

The use of 10 wires on each side of the pier would require the drilling of 20 holes. This was considered excessive damage to the monument, therefore it was decided to connect two wires on a rigid pipe, which was in turn connected to one steel strand. This resulted in a decrease of the required holes from 20 to only 10.

Fig. 9 shows 10 of the wires hanging from the rigid base at the top of the pier. Every two wires are connected to a steel pipe which is in turn connected to one steel strand. Each of the strands is connected to two prestressing devices, which are placed in series (Fig. 10), which is anchored on a bolt at the bottom of the pier (Figs. 10 and 11).

Having setup all twenty wires, tensioning of the wires took place in a symmetric manner. First the

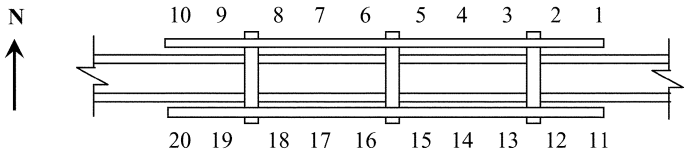

Fig. 12 Plan view of the top support showing the numbering of the SMA wires

Table 1 Strains in the loaded wires

Wire No	Initial Length (cm)	Final Length (cm)	Strain (%)	Wire No.	Initial Length (cm)	Final Length (cm)	Strain (%)
1	53.5	55.0	2.80	11	53.8	54.5	1.30
2	51.6	53.6	3.88	12	54.2	55.2	1.85
3	51.0	52.1	2.16	13	52.1	53.2	2.11
4	52.1	52.9	1.54	14	53.1	54.0	1.69
5	52.5	53.5	1.90	15	53.0	54.3	2.45
6	52.5	53.9	2.67	16	54.0	55.6	2.96
7	53.0	53.5	0.94	17	52.0	53.0	1.92
8	52.3	53.0	1.34	18	53.0	54.3	2.45
9	53.0	53.8	1.51	19	53.3	54.0	1.31
10	53.5	54.8	2.43	20	53.8	54.9	2.04
		Average strain	2.12			Average Strain	2.01

four central wires were tensioned. At first the prestressing devices were used to remove any slack that existed in the assembly. When that was done, the initial length of the SMA devices was measured, as shown in Fig. 9. This length was used to calculate the strain in the wire as the tensile force was increased by turning the prestressing devices. Based on the data in Fig. 4 it was decided that a 2% strain would be applied in the SMA wires since that constituted the center of the plateau.

As it can be observed from Fig. 9 only two of the SMA wires (on each side of the pier) appear to be stretched since the experiment started by applying a prestressing force to only 4 of the 20 wires (wire no. 5, 6, 15 and 16 in Fig. 12). Two more measurements were taken and in each case 8 more wires (4 on each side) were prestressed giving a total of 12 and 20 wires, respectively, by stressing first wires no. 1, 2, 9, 10, 11, 12, 19 and 20, and then wires no. 3, 4, 7, 8, 13, 14, 17 and 18. Then an unloading cycle took place by removing first the central 4 wires (wires no. 5, 6, 15 and 16) resulting in a 16 wire loading and then removing 8 more wires (wires no. 1, 2, 9, 10, 11, 12, 19 and 20) resulting in an 8 wire loading.

The length measurements and the strain calculations for the loading phase are shown in Table 1. It should be noted that during unloading no measurements were taken since from checks that were made, there was insignificant change in the length of the loaded wires when either the number of loaded wires was increased or decreased. It can be observed from the table that wire no. 11 has a small strain. This is due to the fact that the thread of the prestressing device failed and no additional load could be applied. Although it was very difficult to reach the 2% strain in all the wires, an attempt was made to have the strains between 1% and 3%. As it can be seen from the table on the average the strain in the wires at each side of the pier was very close to 2%.

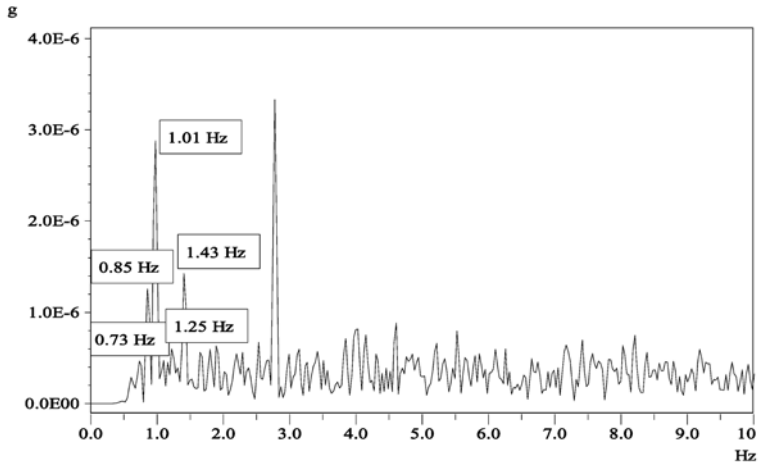

Fig. 13 FFT for position 1 (Fig. 14)

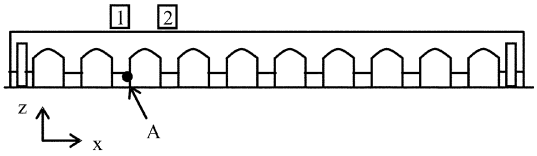

Fig. 14 Location of accelerometers and excitation

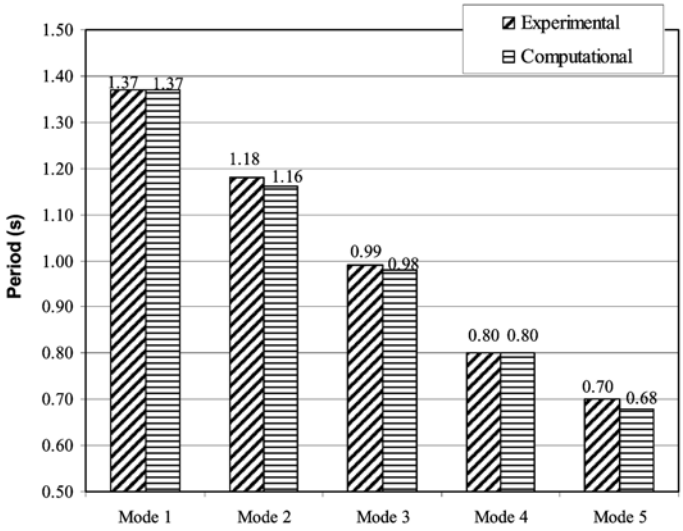

Fig. 15 Comparison between measured and calculated periods of vibration

5. System identification

5.1. Measurements and computational model without SMA devices

Chrysostomou, *et al*. (2004) and (2008), describe the methodology used for obtaining the dynamic

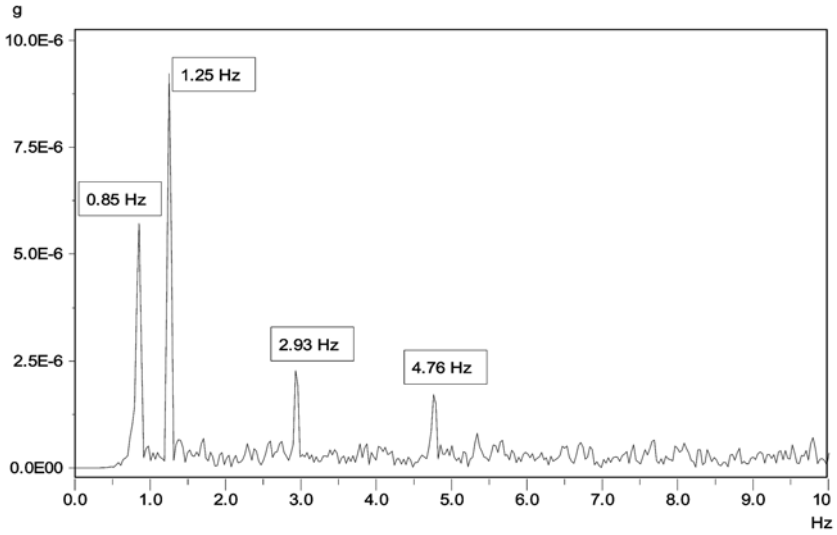

Fig. 16 FFT for position 1 with 4 SMA wires loaded

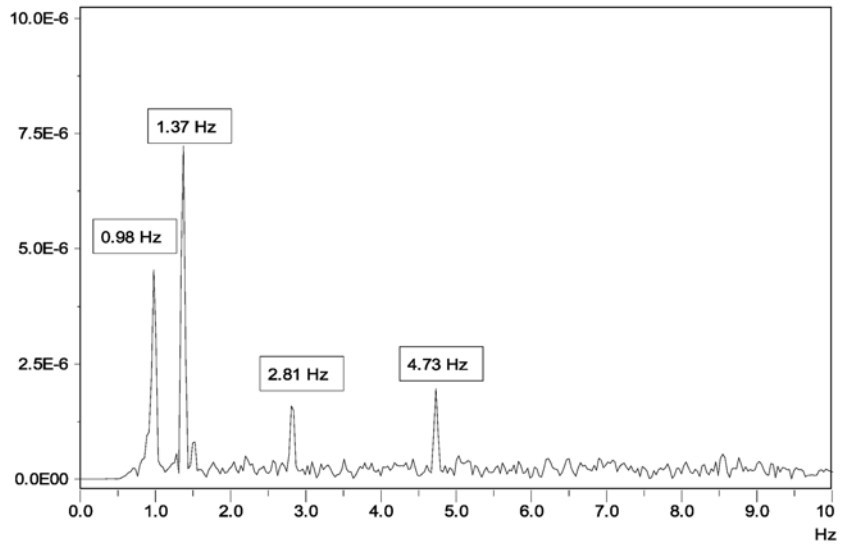

Fig. 17 FFT for position 1 with 12 SMA wires loaded

characteristics of the monument and the development of a computational model. Fig. 13 shows the FFT obtained from the signal analysis and the first five frequencies that were identified. The signals were obtained from two triaxial accelerometers (EpiSensors) positioned at 2 different locations on the aqueduct indicated with numbers 1 and 2 in Fig. 14.

Chrysostomou, *et al*. (2008) also describe the development of a computational model to simulate the behaviour of the aqueduct. The eigenvalue analysis of the model resulted in the following periods of vibration: 1.37 s, 1.16 s, 0.98 s, 0.80 s and 0.68 s. The comparison of the measured and computed periods of vibration for the first five modes is shown in Fig. 15. It should be noted that there is a very close agreement between the calculated and the measured periods of vibration.

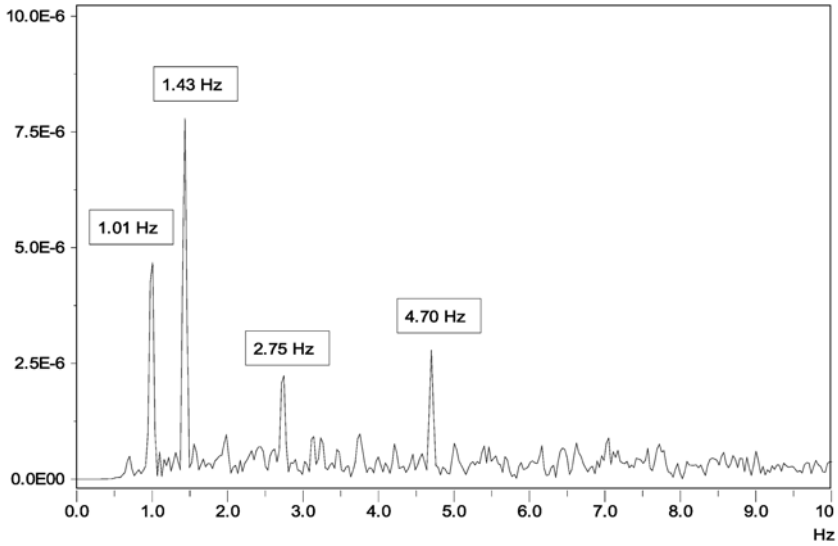

Fig. 18 FFT for position 1 with 20 SMA wires loaded

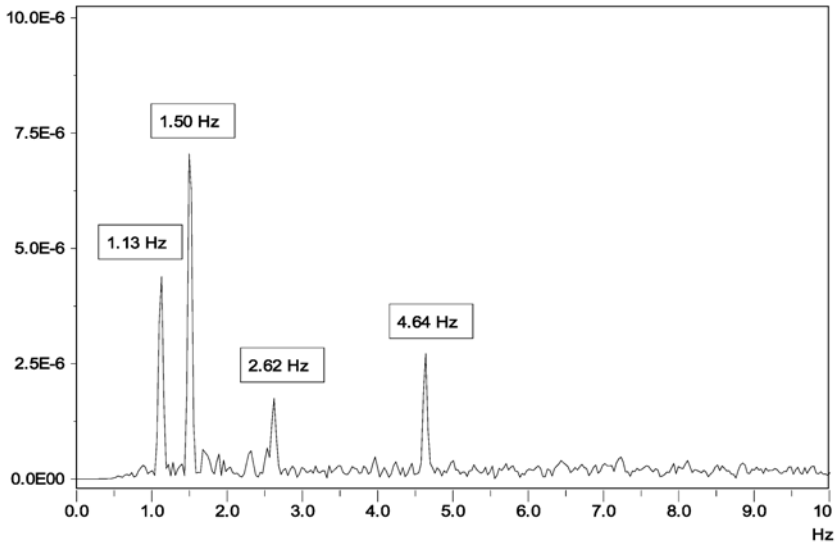

Fig. 19 FFT for position 1 with 16 SMA wires loaded

5.2. Measurements with SMA wires

Two EpiSensors were positioned at 2 different locations on the aqueduct indicated with numbers 1 and 2 (see Fig. 14), and a rubber impact hammer was used to induce vibrations in the aqueduct in addition to ambient vibrations. One impact location was used indicated in Fig. 14 with the letter A. The x-axis, y-axis and z-axis of the EpiSensors were aligned with the longitudinal, perpendicular to its plane and vertical directions of the aqueduct, respectively.

The measurements were analyzed using the software DaisyLab 9.0. A Fast Fourier Transform (FFT) was used with a low pass Butterworth filter of 10 Hz, a high pass Butterworth filter of 0.6 Hz and a

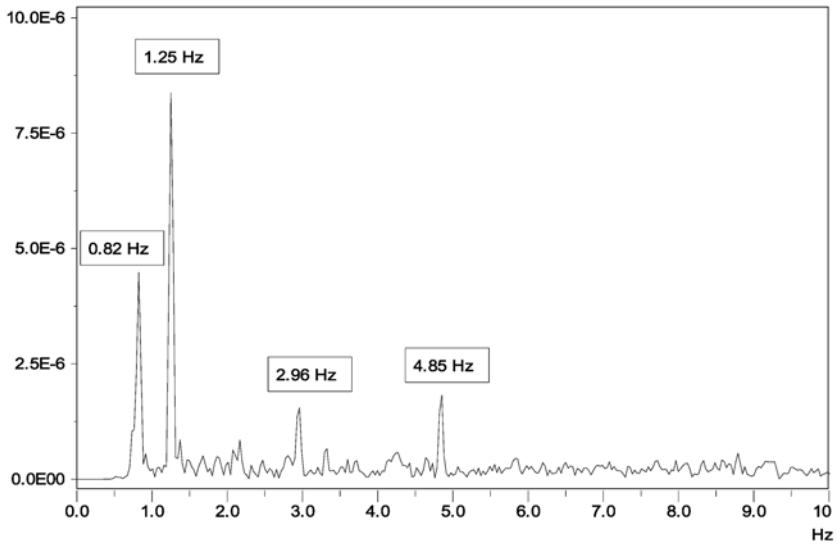

Fig. 20 FFT for position 1 with 8 SMA wires loaded

Table 2 Measured frequencies for the various loading cases

Loading Cycle	Loading			Unloading	
No. of wires	4	12	20	16	8
Frequency 1 (Hz)	0.85	0.98	1.01	1.13	0.82
Frequency 2 (Hz)	1.25	1.37	1.43	1.50	1.25
Frequency 3 (Hz)	2.93	2.81	2.75	2.62	2.96
Frequency 4 (Hz)	4.76	4.73	4.70	4.64	4.85

Hanning data window.

As explained in the previous section, five loading conditions were applied on the structure by prestressing 4 wires, 12 wires and 20 wires in a loading cycle, and then by removing the load in 4 wires, hence leaving 16 wires loaded, and finally removing 8 wires leaving 8 wires loaded. The results of the FFT analysis of the signal at position 1 are shown in Figs. 16 to 20. It should be noted that the same results were obtained by the sensor which was placed at position 2.

6 Discussion of the results

In comparing Figs. 16 to 20 with Fig. 13 it is obvious that the application of the SMA wires have a significant effect on the dynamic behaviour of the aqueduct. While in the case that there are no wires on the structure the obtained signal is complex and only a few distinct frequencies appear, as soon as the SMA wires are applied, the signal in all the cases clears-up and four distinct frequencies appear. It is obvious that there may exist additional frequencies between these distinct frequencies and in particular between the second and the third and the third and the forth ones, but since there is no means to establish them in a definite way, then no attempt is made to report any of those.

The results presented in Figs. 16 to 20 are summarized in Table 2. It is obvious from the results that as

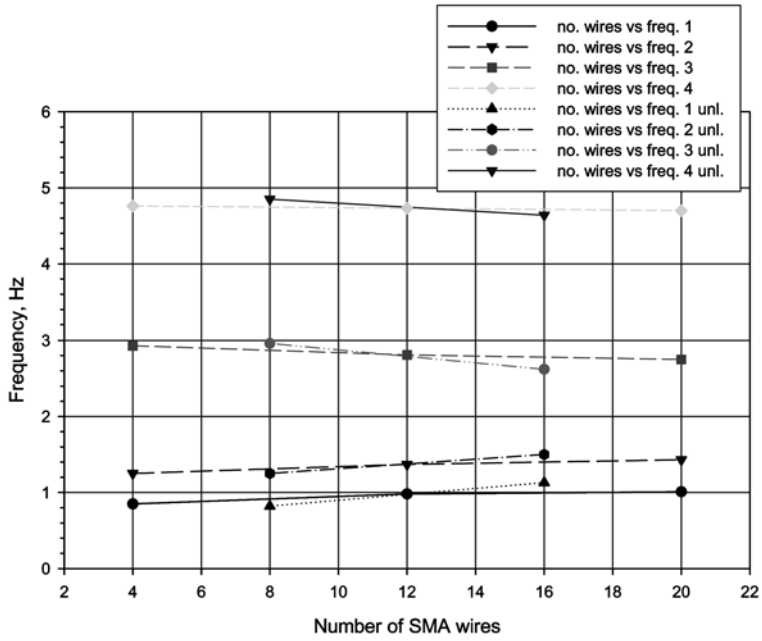

Fig. 21 Variation of the measured frequencies with the number of SMA wires for the loading and unloading (unl.) cycles

the number of wires increases from 4 to 20, there is a shift of the fundamental frequency from 0.85 Hz to 1.01 Hz (period shift from 1.18 s to 0.99 s). The same is observed for the second recorded frequency. This indicates a stiffening of the structure due to the application of a prestressing force. This stiffening can be explained by the increase in contact between the masonry units and hence the increase of its stiffness through the increase of the modulus of elasticity of the masonry matrix. For the third and the forth frequencies though a slight decrease is recorded with the increase of the number of wires, from 2.93 Hz to 2.75 Hz and from 4.76 Hz to 4.70 Hz, respectively.

In the case of unloading, the same behaviour is exhibited by the structure. For the first two recorded frequencies, as the number of wires decreases from 16 to 8 there is a decrease in the measured frequency, which indicates softening of the structure due to the removal of a prestressing force and hence decrease of the effective modulus of elasticity of the masonry matrix. For the other two frequencies the reverse takes place; that is as the number of wires decreases the measured frequencies increase slightly.

A discrepancy appears to exist between the results for the 20 wires compared to those for the 16 wires. Although the prestressing force is decreased, the magnitude of the first two measured frequencies increases, while that of the other two decreases. An explanation for this can be the difference in the load pattern that was applied due to the difference in the sequence of prestressing the wires as explained under the section of experimental setup. By removing the four wires in the middle to go from the 20 to the 16 wires in the unloading cycle, a different load pattern was formed compared to the loading one, in which the four middle wires were the first to load. Therefore, since there was a difference in the loading distribution then the loading and unloading cycles should be treated as distinct cases.

The results presented in Table 2 and discussed above are plotted in Fig. 21. From the figure it is obvious that the increasing slope for frequencies 1 and 2 for the loading cycle is the same, while the

Table 3 Load in the wires

Wire No.	Strain (%)	Stress (N/mm^2)	Load (kN)	Loading case 1 (kN)	Loading case 2 (kN)	Loading case 3 (kN)	Loading case 4 (kN)	Loading case 5 (kN)
1	2.80	173.5	1.669		1.669	1.669	1.669	
2	3.88	195.9	1.885		1.885	1.885	1.885	
3	2.16	160.7	1.546			1.546	1.546	1.546
4	1.54	147.8	1.422			1.422	1.422	1.422
5	1.90	155.4	1.495	1.495	1.495	1.495		
6	2.67	170.9	1.644	1.644	1.644	1.644		
7	0.94	133.5	1.284			1.284	1.284	1.284
8	1.34	143.2	1.378			1.378	1.378	1.378
9	1.51	147.1	1.415		1.415	1.415	1.415	
10	2.43	116.2	1.118		1.118	1.118	1.118	
11	1.30	142.2	1.368		1.368	1.368	1.368	
12	1.85	154.3	1.485		1.485	1.485	1.485	
13	2.11	159.7	1.536			1.536	1.536	1.536
14	1.69	151.0	1.453			1.453	1.453	1.453
15	2.45	166.6	1.603	1.603	1.603	1.603		
16	2.96	176.6	1.699	1.699	1.699	1.699		
17	1.92	155.6	1.497			1.497	1.497	1.497
18	2.45	166.6	1.603			1.603	1.603	1.603
19	1.31	142.5	1.371		1.371	1.371	1.371	
20	2.04	158.3	1.523		1.523	1.523	1.523	
			Total Load	6.441	18.275	29.995	23.553	11.719

Table 4 Load in the wires and corresponding frequencies

Loading Cycle	Loading			Unloading	
No. of wires	4	12	20	16	8
Load in wire cluster (kN)	6.441	18.275	29.995	23.553	11.719
Frequency 1 (Hz)	0.85	0.98	1.01	1.13	0.82
Frequency 2 (Hz)	1.25	1.37	1.43	1.50	1.25
Frequency 3 (Hz)	2.93	2.81	2.75	2.62	2.96
Frequency 4 (Hz)	4.76	4.73	4.70	4.64	4.85

decreasing slope for frequencies 3 and 4 is also the same. The exact same pattern is observed for the unloading cycle with a slight difference in the slopes of the lines.

Since the strain in the wires is not the same (Table 1), then the loading in the wires is also different. This means that plotting the variation of frequencies as a function of the number of wires may not give meaningful results. Using the data in Table 1 and the stress-strain relationship of Fig. 3, the load in each of the 3.5 mm diameter wires were calculated as shown in Table 3. Then the total load for each of the loading cases was calculated by adding the loads in the participating wires. The results of this calculation are shown in Table 4 and the plots of the frequencies versus the load in the SMA wires are

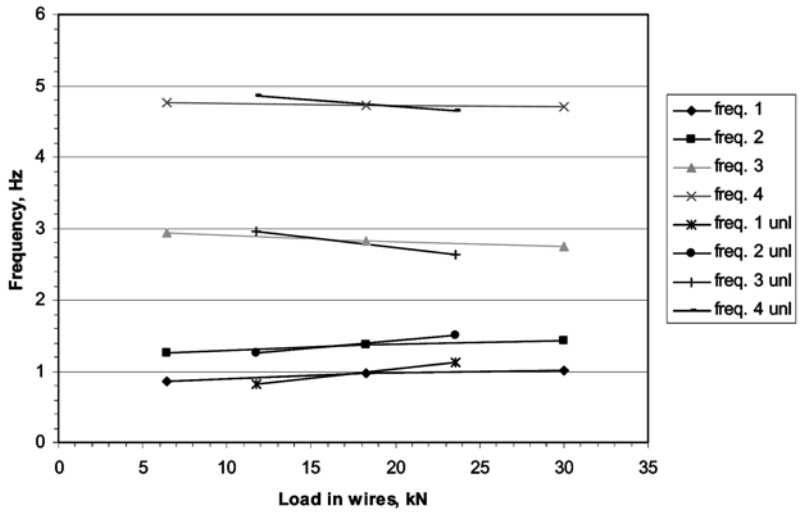

Fig. 22 Variation of the measured frequencies with the load in clusters of SMA wires for the loading (4, 12, 20 wires) and unloading (unl., 16, 8 wires) cycles

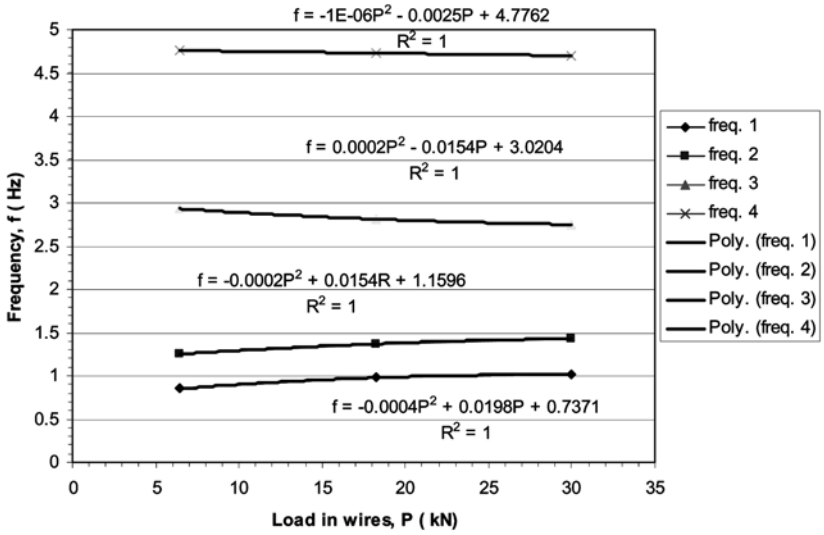

Fig. 23 Fitted curves of the variation of the measured frequencies with the load in clusters of SMA wires for the loading (4, 12, 20 wires) cycle

shown in Fig. 22.

In comparing Figs. 21 and 22 it can be observed that they give the same trends, although there may be some difference in the slopes of the curves. Therefore it can be stated that provided that there is not a large variation in the strains in the loaded wires, the plots of frequency versus wire number and frequency versus load, give similar results.

Using now the results shown in Fig. 22 for the loading cycle, second order polynomials were fitted to the results as shown in Fig. 23. From the equation for the fundamental frequency, it can be predicted that the fundamental frequency of the structure when no wires are applied is 0.737 Hz. This

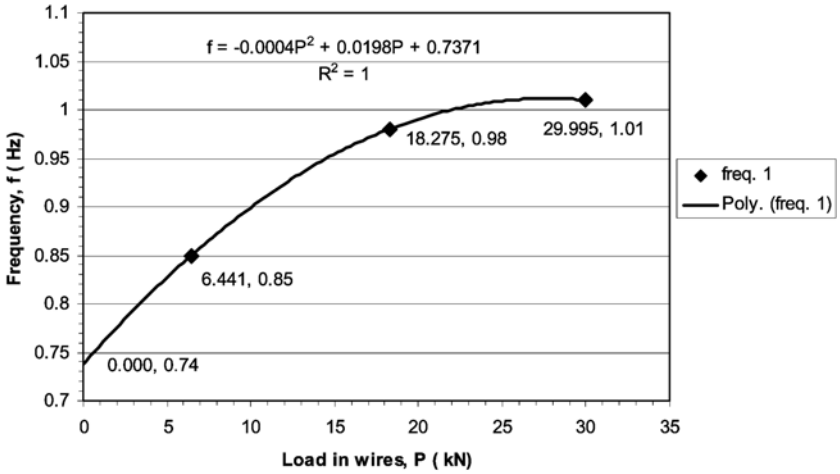

Fig. 24 Extrapolation of the fitted curve of the 1st frequency to zero-load for the loading (4, 12, 20 wires) cycle

is shown in Fig. 24, in which the fitted line was used to extrapolate backwards to zero load at which the intercept is 0.74 Hz. In comparing with the measured fundamental frequency of the structure (Fig. 13), it is obvious that there is a close match and therefore this equation can be used for the prediction of the modification of the fundamental frequency of the structure as a function of the applied load in the SMA wires.

7. Conclusions

In this paper the results of the application of copper-based shape-memory-alloy prestressing devices on an ancient aqueduct are presented. The dynamic characteristics of the monument without the application of SMA are reported by Chrysostomou, *et al*. (2008).

From the measurements it is clear that the SMAs have a significant effect on the dynamic characteristics of the monument. It was observed that the application of the wires had as a result the significant modification of the recorded signal. While for the case of no wires the signal was rather complicated, the application of the wires had as an effect the clearing of the signal and the recording of 4 predominant frequencies, irrespective of the number of wires applied.

Certain trends were also recorded. As the number of the wires increased, the first two recorded frequencies have also increased, while a slight decrease was recorded for the 3rd and 4th frequencies. A similar trend was noted in the case of unloading of the wires, but now a decrease in the recording frequency with a decrease in the number of wires was observed for the first two recorded frequencies and an increase for the last two.

The increase in the fundamental frequency from 0.85 Hz to 1.01 Hz (period shift from 1.18 s to 0.99 s) shows an increase in the stiffness of the structure, which can be attributed to modification of the modulus of elasticity due to the prestressing force that makes the masonry matrix more homogeneous.

A discrepancy was observed between the loading and the unloading cycle. An explanation for this can be the difference in the load pattern that was applied due to the difference in the sequence of prestressing the wires as explained under the section of experimental setup.

Plotting frequencies as a function of the number of wires or the load in the wire cluster give the same trends, although there may be some difference in the slopes of the curves. Therefore it can be stated that provided that there is a small variation in the strains in the loaded wires, the plots of frequency versus wire number and frequency versus load, give similar results.

The 2nd order polynomial that was fitted by linear regression in the variation of the fundamental frequency with the load in the wire cluster has resulted in an equation which when extrapolated to zero-load predicted a frequency of 0.74 Hz, which is the one measured on the structure without any wires. This equation can be, therefore, used for the prediction of the modification of the fundamental frequency of the structure as a function of the applied load in the SMA wires.

Based on the above findings it can be concluded that the application of the SMA wires on a real structure has shown that they significantly change the dynamic characteristics of the structure. This is a matter that should be further investigated by laboratory tests in order to establish the relationship between the variation of the frequencies of the structure and the modulus of elasticity of the masonry matrix. This relationship should then be tested by the development of a computational model that will be able to predict the behaviour of the aqueduct when the SMA prestressing devices are applied, and hence investigate numerically the effectiveness of the SMA wires in the protection of monuments from earthquakes.

Acknowledgments

The authors acknowledge the financial contribution of the European Commission through the project Wide-Range Non-Intrusive devices toward Conservation of Historical Monuments in the Mediterranean Area (WIND-CHIME) and the cooperation of Ing. Mauro Mottini for the design of the tie anchorage. The authors are also thankful to Professor Fabio Casciati, coordinator of the project. We would also like to express our thanks to the Director of the Department of Antiquities of the Republic of Cyprus for giving us permission to apply the SMA devices on the monument, in order to perform the experiment.

References

Auricchio, F. (1995), "Shape memory alloys: applications, micromechanics, macromodelling and numerical simulations", PhD Thesis, University of California at Berkeley, USA.

Auricchio, F., Taylor, R. L., and Lubliner, J. (1997) "Shape-memory alloys: macromodeling and numerical simulations of the superelastic behavior", *Comput. Methods Appl. Mech. Eng.*, **146**, 281-312.

Auricchio, F., Faravelli, L., Magonette, G. and Torra, V. (eds.) (2001), "Shape memory alloys: advances in modelling and applications", *CIMNE*, Barcelona.

Biritognolo, M., Bonci, A. and Viskovic, A. (2000), "Numerical models of masonry façade walls with and without SMADs", *Proc. Final Workshop of ISTECH Project – Shape Memory Alloy Devices for Seismic Protection of Cultural Heritage Structures*, 117-140, Joint Research Centre, Ispra, Italy, June.

Buehler, W. J. and Wiley, R. C. (1965), "Nickel-based alloys", *Technical report*, US-Patent 3174851.

Casciati, F. (ed.) (2003), *Proceeding of the 3rd World Conference on Structural Control*, John Wiley & sons, Chichester.

Casciati, F. and Faravelli, L. (2004), "Experimental characterisation of a cu-based shape memory alloy toward its exploitation in passive control devices", *Journal de Physique IV*, **115**, 299-306.

Casciati, S. and Faravelli, L. (2003), "Thermo-mechanic properties of a cu based shape memory alloy", *Proceedings SMART03*, Poland.

Casciati, S. and Faravelli, L. (2004a), "Thermo-mechanic characterization of a cu-based shape memory alloy", *Proceedings SE04*, Osaka, Japan, 377-382.
Casciati, S. and Faravelli, L. (2004b), "Fastening cracked blocks by SMA devices", *Proceedings of the 3rd European Conference on Structural Control*, Vienna, Austria, M1-1/M1-4.
Casciati, S., Faravelli, L. and Domaneschi, M. (2005), "Dynamic tests on Cu- based shape memory alloys toward seismic retrofit of cracked stone monuments", *Workshop on Smart Structures and Advanced Sensor Technologies*, June 26-28, Santorini Greece.
Casciati, S. and Osman, A. (2005), "Damage assessment and retrofit study for the luxor memnon colossi", *J. Struct. Cont. Health Monit.*, **12**, 139-159.
Chrysostomou, C. Z. Demetriou, Th. and Pittas, M. (2002), "Conservation of historical Mediterranean sites by innovative seismic-protection techniques", *Proceedings 3rd World Conference on Structural Control*, **2**, 947-954, Como, Italy, April 7-12.
Chrysostomou, C. Z., Demetriou, T. and Stassis, A. (2004), "Seismic protection of an aqueduct by innovative techniques", *Proceedings 3rd European Conference on Structural Control*, Vienna, July.
Chrysostomou, C. Z., Demetriou, T., Pittas, M. and Stassis, A. (2005), "Retrofit of a church with linear viscous dampers", *J. Struct. Cont. Health Monit*, **12**(2), 197-212, April/June.
Chrysostomou, C. Z., Demetriou, and Stassis, A. (2008), "Health-monitoring and system-identification of an ancient aqueduct", *Smart Struct. Sys.*, **4**(2), 183-194.
Croci, G. (2000), "General methodology for the structural restoration of historic buildings: the cases of the tower of pisa and the basilica of assisi", *J. Cultural Heritage*, **1**, 7-18.
Delmonte, G. (2007), "Pretensionamento con fili in lega a memoria di forma di elementi strutturali murari", Master Thesis, Department of Structural Mechanics, University of Pavia, Italy, (in Italian).
Faravelli, L. and Casciati, S. (2003), "Dynamic behavior of a shape memory alloy structural devices: numerical and experimental investigation", K. Watanabe and F. Ziegler (eds.), *Dynamics of Advanced Materials and Smart Structures*, IUTAM series, Kluwer Academic Publishers, Dordrecht, Netherlands, 63-72.
Isalgue, A., Torra, V. and Lovey, F. C. (2002), "Cu-based SMA: quantifying and guaranteeing the time and temperature dependence on damping", F. Casciati (ed.), *Proceedings of the 3rd Word Conference on Structural Control*, Vol. **2**, John Wiley & sons, Chichester, UK, 363-368.
Saadat, S., Salichs, J., Noori, M., Hoo, Z., Davoodi, H., Bar-on, I, Suzuki, Y. and Masuda, A. (2002), "An overview of vibration and seismic application of NiTi shape memory alloys", *Smart Mater. Struct.*, **11**(2), 218-229.
SmartLab, http://smart.tamu.edu/, accessed on may 2007.

FC